International Journal of Biological Macromolecules 129 (2019) 715–727

Contents lists available at ScienceDirect

International Journal of Biological Macromolecules

journal homepage: http://www.elsevier.com/locate/ijbiomac

Use of cellulose acetate/polyphenylsulfone derivatives to fabricate ultrafiltration hollow fiber membranes for the removal of arsenic from drinking water

Mithun Kumar [a], Somasekhara RaoT. [a,**], Arun M. Isloor [b,**], G.P. Syed Ibrahim [b], Inamuddin [d,e,f,*], Norafiqah Ismail [c], Ahmed Fauzi Ismail [c], Abdullah M. Asiri [d,e]

[a] Department of Mechanical Engineering, National Institute of Technology Karnataka, Surathkal, Mangalore 575 025, India
[b] Membrane Technology Laboratory, Department of Chemistry, National Institute of Technology Karnataka, Surathkal, Mangalore 575 025, India
[c] Advanced Membrane Technology Research Center (AMTEC), Universiti Teknologi Malaysia, 81310 Skudai, Johor Bahru, Malaysia
[d] Chemistry Department, Faculty of Science, King Abdulaziz University, Jeddah 21589, Saudi Arabia
[e] Centre of Excellence for Advanced Materials Research, King Abdulaziz University, Jeddah 21589, Saudi Arabia
[f] Advanced Functional Materials Laboratory, Department of Applied Chemistry, Faculty of Engineering and Technology, Aligarh Muslim University, Aligarh 202 002, India

ARTICLE INFO

Article history:
Received 15 October 2018
Received in revised form 11 January 2019
Accepted 3 February 2019
Available online 06 February 2019

Keywords:
Polyphenylsulfone
Cellulose acetate
Cellulose acetate phthalate
Hydrophilicity
Ultrafiltration
Arsenic removal

ABSTRACT

Cellulose acetate (CA) and cellulose acetate phthalate (CAP) were used as additives (1 wt%, 3 wt%, and 5 wt%) to prepare polyphenylsulfone (PPSU) hollow fiber membranes. Prepared hollow fiber membranes were characterized by surface morphology using scanning electron microscopy (SEM), surface roughness by atomic force microscopy (AFM), the surface charge of the membrane was analyzed by zeta potential measurement, hydrophilicity by contact angle measurement and the functional groups by fourier transform infrared spectroscopy (FTIR). Fouling resistant nature of the prepared hollow fiber membranes was evaluated by bovine serum albumin (BSA) and molecular weight cutoff was investigated using polyethylene glycol (PEG). By total organic carbon (TOC), the percentage rejection of PEG was found to be 14,489 Da. It was found that the hollow fiber membrane prepared by the addition of 5 wt% of CAP in PPSU confirmed increased arsenic removal from water as compared to hollow fiber membrane prepared by 5 wt% of CA in PPSU. The removal percentages of arsenic with CA-5 and CAP-5 hollow fiber membrane was 34% and 41% with arsenic removal permeability was 44.42 L/m^{2}h bar and 40.11 L/m^{2}h bar respectively. The increased pure water permeability for CA-5 and CAP-5 hollow fiber membrane was 61.47 L/m^{2}h bar and 69.60 L/m^2 h bar, respectively.

1. Introduction

Nowadays, because of urbanization and industrialization water bodies are getting polluted by different types of heavy metals and metalloids like arsenic. Consumption of arsenic contaminated water is causing a major threat to the public and affecting millions of population in the world. Arsenic-containing pollutants are continuously releasing from natural sources such as biological activities, volcanic emissions, weathering and so on. The anthropogenic sources such as fossil fuel combustion, non-ferrous smelting, petroleum refinery and gold mining are also responsible for the release of arsenic into water bodies. Arsenic contamination can cause a serious health hazard to humankind [1]. As far as human health is concerned, the presence of arsenic in water leads to cancer, heart diseases, numbness, darkening of skins, encephalopathy, abdominal pain and vomiting [2]. In order to overcome these health hazards arises from arsenic, the National Water Commission in Mexico government has employed at a time 200 reverse osmosis membrane systems for arsenic removal from water [3]. However, there are many technologies used, such as adsorption [4,5], ion exchange [6,7], coagulation [8] and membrane technology [9]. Among these technologies, membrane-based filtration is a preferred technology to remove arsenic contamination from water due to its high efficiency, low energy consumptions and high filtration performance [10].

Ultrafiltration, nanofiltration and reverse osmosis is a favorable classification for pressure-driven membrane filtration processes for arsenic removal from water. A lot of research work is ongoing for removing the arsenic from water, Briefly, Rezaee et al. [11] prepared polysulfone (PSf) and graphene oxide blended membranes for estimation of arsenic rejection from the water. Increase in concentration of graphene oxide in PSf could increase the rejection percentage and enhance hydrophilicity, flux

* Correspondence to: Inamuddin, Chemistry Department, Faculty of Science, King Abdulaziz University, Jeddah 21589, Saudi Arabia.
** Corresponding authors.
E-mail addresses: ssrao@nitk.edu.in (S. RaoT.), isloor@yahoo.com (A.M. Isloor), inamuddin@rediffmail.com (Inamuddin).

https://doi.org/10.1016/j.ijbiomac.2019.02.017
0141-8130/

and porosity. In another study, He et al. [12] used PSf along with zirconium nanoparticles for fabrication of hollow fiber membranes using non-solvent induced phase separation process. These hollow fiber membranes were effective for removal of arsenic from 51.65 ppm to 92.65 ppb in the pH range of 2–9. Gohari et al. [13] prepared membranes using a novel polyethersulfone (PES) with Fe/Mn as binary oxide particles for arsenic removal from arsenic contaminated water by ultrafiltration process. Song et al. [14] used PES hollow fiber membranes coated with sulfonated poly (ether ether ketone) for arsenic removal from contaminated water. Chatterjee et al. [15] prepared hollow fiber membranes from polyacrylonitrile impregnated laterite and polyvinylpyrrolidone as an additive for arsenic removal from ground-water by the ultrafiltration process [16].

Cellulose acetate (CA) membranes are effectively utilized for arsenic rejection from water [17]. Terrazasbandala et al. [18] fabricated cellulose triacetate (CTA) and activated carbon membranes using a solvent casting method for arsenic removal (45%). Nevárez and group members [3] enhanced arsenic removal by improving surface adsorptivity from the ultrafiltration process of prepared bio-eco-friendly nanocomposite membranes from non-solvent induced phase separation technique using propionate lignin (kraft, hydrolytic and organosolve) along with CTA. Jayalakshmi et al. [19] fabricated CA poly-isophthalamide-*graft*-methacrylamide (CA/PIPA-g-MAA) mixed asymmetric ultrafiltration membranes for arsenic removal from water.

Cellulose acetate phthalate (CAP) as an effective additive has also been used for the removal of fluoride, different dyes, and heavy metals from ground-water. Moreover, CAP belongs to cellulose ester groups and is well known to form a hydrogen bond because it contains a C═O and –OH group [20]. Seidel et al. [21] concluded that the removal of arsenic using membrane technology mainly depends on surface charge, solution concentration, solution temperature, solution pH, compositions used for membrane preparation and operating temperature. From the above literature, it was clear that CAP was identified as a good additive for the arsenic removal. In view of the efficiency and performance of the membranes, hollow fiber membranes are more superior as compared to the flat sheet membranes [22–24]. An overview of the literature indicated no any research work was done using CAP hollow fiber membranes for arsenic removal from water.

Many researchers were successful in incorporating CA as an adsorbing agent. CA is mostly used as low -cost ultrafiltration additive which is known for its hydrophilicity, moderate flux, adsorption property and renewable sources in nature [25,26]. However, pure CA hollow fiber membranes possess several drawbacks such as lack of chemical, biological and mechanical stability as they are very brittle in nature. Hence, such drawbacks have limited the CA membranes in arsenic rejection application [18]. The composition of CA with a different polymer and the addition of a small percentage of additives is a promising blending method to enhance the properties of prepared membranes [27,28]. In our study, as-used PPSU exhibited better characteristics as compared to other polymers in terms of remarkable physical and chemical properties, high glass transition temperature, better mechanical properties and resistance towards hydrolysis [29,30]. Due to these benefits, PPSU has frequently used polymer for ultrafiltration, nanofiltration and reverse osmosis processes [31–33].

According to our perceptions, hollow fiber membranes prepared from polyphenylsulfone along with cellulose acetate and cellulose acetate phthalate as additives were still not yet been studied for arsenic removal applications. To satisfy the above requirement, it was proposed to fabricate hollow fiber membranes to remove arsenic from water. For the first time, we have introduced cellulose acetate phthalate/polyphenylsulfone hollow fiber membranes for arsenic removal from drinking water. The main aim of this study is to fabricate, characterize and compare the arsenic removal efficiency from prepared hollow fiber membranes.

2. Materials and methods

Polyphenylsulfone (PPSU, molecular weight (MW) of 50,000 g/mol, Radel R-5000) was purchased from Solvay advanced polymer (Belgium). *N*-Methyl-2-pyrrolidone and arsenic standard solution 1000 mg/L were procured from Merck, India. Cellulose acetate powder (Mw 50000 with acetylene content 39.7 wt%), cellulose acetate phthalate (Mw 2534.12), bovine serum albumin and polyethylene glycol of different molecular weights as 6000, 10,000 and 20,000 g/Mol were procured from Sigma-Aldrich, India. All polymers were dried in an oven for overnight at 50 °C.

2.1. Preparation of cellulose acetate/polyphenylsulfone, cellulose acetate phthalate/polyphenylsulfone hollow fiber membranes

Polyphenylsulfone and cellulose acetate hollow fiber membranes were prepared by the dry-wet spinning method at room temperature. CA was dissolved in *N*-Methyl-2-pyrrolidone and stirred properly to get a homogeneous solution. PPSU was added to obtain the dope solution. The further homogeneous dope solution was obtained by allowing it to mechanical stirring for about 24 h at 60 °C. This homogeneous solution was subjected to the sonication process for the removal of trapped air bubbles present in the solution [29,34]. The same procedure was used for the preparation of CAP and PPSU hollow fiber membranes. Different compositions of the prepared dope solution were illustrated in Table 1.

The prepared homogeneous dope solution was allowed to pass through the spinneret of dimensions 1.1/0.55 mm (outer diameter/inner diameter) under nitrogen gas pressure. Reverse osmosis water was used as bore fluid and guided to pass through adjacent sides of the spinneret. With the help of a gear pump, the dope solution at the top and the bore fluid at the adjacent sides were allowed to pass through the spinneret. The detailed parameters used for spinning of prepared dope solution were illustrated in Table 2. The air gap distance between the spinneret plate and water contact in the coagulation bath was maintained at 4 cm. This region is a very important region because the formation of hollow fiber membrane takes place with the aid of the phase inversion method. Continuously formed hollow fiber membranes were wound on a rotating drum. Prepared hollow fiber membranes were then kept in water for 24 h and 10 wt% of glycerol solution for another 24 h to avoid hollow fiber pore shrinkage. Finally, the obtained hollow fiber membranes were dried at room temperature.

2.2. Characterization of cellulose acetate/polyphenylsulfone, cellulose acetate phthalate/polyphenylsulfone hollow fiber membranes

2.2.1. Surface morphologies of hollow fiber membranes

Scanning electron microscopy (SEM) Hitachi TM3000 was used to characterize the cohesive and surface morphology of the hollow fiber membranes. Dried hollow fiber membranes were dipped in methanol solution for 3 min to avoid surface charging of the membranes, further membranes were fractured in liquid nitrogen (cryogenic) bath, where the membrane surfaces were frozen to get smooth uniform surfaces. After cryogenic treatment, with the help of EMITECH K575 sputter

Table 1
Compositions for membrane preparation.

Membrane	PPSU (g)	NMP (g)	CA (g)	CAP (g)
Neat membrane	14	86	0	–
CA-1	14	85.9	0.1	–
CA-3	14	85.7	0.3	–
CA-5	14	85.5	0.5	–
CAP-1	14	85.9	–	0.1
CAP-3	14	85.7	–	0.3
CAP-5	14	85.5	–	0.5

Table 2
Spinning parameters for preparation of hollow fiber membrane.

Parameter	Condition
Spinneret OD/ID (mm)	1.1/0.55
Dope solution	PPSU/CA/NMP and PPSU/CAP/NMP
Dope extrusion rate (mL/min)	3.5
Bore fluid	RO water
Bore flow rate (mL/min)	2.5
Air gap (cm)	4
Treatment bath	Water
Coagulation bath temperature	26 °C
Drum speed (rpm)	13
Gear pump speed (rpm)	10

coater, the hollow fiber membrane surfaces were sputter coated with platinum [35].

2.2.2. Hydrophilicity of hollow fiber membranes

Surface hydrophilicity of hollow fiber membranes was investigated using FTA-200 dynamic contact angle measurement, sessile droplet method. The neat membrane, CA/PPSU and CAP/PPSU –hollow fiber membranes were tested and deionized water was used as probe liquid, the source of light was focused on one side of the instrument on hand camera and hand camera was provided to take an image of the bubble on the surface of the membrane. The contact angle was measured at three different places and the average value was reported. The better affinity between the water droplet and the surface of the membrane results in a smaller contact angle which further enhances surface hydrophilicity [36,37].

2.2.3. Pure water permeability of hollow fiber membranes

Using cross-flow filtration cell, investigations of pure water permeability of neat and blended –hollow fiber membrane was carried out. Five favorable membranes with the desired length of 10 cm were taken from prepared hollow fiber membrane modules. The membranes were potted using stainless steel holder, prior to potting, a composition blend of epoxy resin and hardener from Loctite EA E-30CL adhesive was prepared in the proportion of 2:1 for holding the membranes in stainless steel, and allowed to dry for 24 h. With the aid of a cross flow system of filtration, holder along with membrane was kept in membrane cell and fixed properly. With the help of a centrifugal pump, water circulated throughout the system. The pressure gauge was attached to a system such that, the pressure of water in the system can be controlled effectively [38]. Initially, membranes were kept for compaction at 0.4 MPa and 25 °C for 30 min. This mode of pressure is called as trans-membrane pressure. Demineralized water was used for the determination of water permeability throughout the experiment. Water permeability was calculated by the Eq. (1).

$$Jw1 = \frac{Q}{n\pi L \Delta P Di} \tag{1}$$

where, 'Jw_1' is permeate flux, 'Q' is volumetric flow rate (mL/min), 'n' is number of hollow fiber membranes, 'Di' is inner diameters of hollow fiber membrane (cm), 'L' is length of hollow fiber membrane (cm) and 'ΔP' is transmembrane pressure (bar) [39].

2.2.4. Antifouling study of hollow fiber membranes

Antifouling performances of prepared hollow fiber membranes were performed as reported elsewhere [38]. In brief, initially, compaction of each membrane was carried out using pure water for 30 min at a trans-membrane pressure of 0.3 MPa. After completion of compaction, the transmembrane pressure was decreased to 0.10 MPa, at this pressure pure water permeability of membranes were noted as (J_{W1}) in terms of L/m^{2}h bar. The bovine serum albumin (BSA) of 800 ppm (0.8 g/L) concentration aqueous solution was used for the study. The permeability of BSA was noted as (J_p) and allowed to pass through the membranes for 80 min. After completion of BSA filtration study, the hollow fiber membranes were thoroughly cleaned with distilled water and determinations of pure water permeability (J_{w2}) of the membranes were carried out in the same procedure [40]. Flux recovery ratio, total fouling ratio, reversible and irreversible fouling of the membranes were calculated using Eqs. (2), (3), (4) and (5), respectively.

$$\text{FRR} = \frac{J_{w2}}{J_{w1}} \times 100 \tag{2}$$

$$\text{Rt}\ (\%) = \frac{J_{w1} - J_p}{J_{w1}} \times 100 \tag{3}$$

$$\text{Rr}\ (\%) = \frac{J_{w2} - J_p}{J_{w1}} \times 100 \tag{4}$$

$$\text{Rir}\ (\%) = \frac{1 - J_p}{J_{w1}} \times 100 \tag{5}$$

where, '*FRR*' is Flux recovery ratio, 'R_t' is total fouling ratio, 'R_r' is reversible fouling, and 'R_{ir}' is irreversible fouling, 'J_{W1}' is pure water permeability, 'J_p' is bovine serum albumin permeability, 'J_{w2}' is permeability after washing with water.

2.2.5. Water uptake and porosity study

Investigation of water uptake study was performed on prepared hollow fiber membranes after analyzing the literature [41]. In this study, the hollow fiber membranes were cut into pieces of a cross-section of 2 × 1 cm (2 cm^2) and both sides of the membranes are closed by applying epoxy resin along with hardener mixture of 2:1 proportion and allowed to dry. The dried hollow fiber membranes were immersed in demineralized water about 24 h. The membranes were taken out from demineralized water and wet weight (W_w) was noted after wiping with a blotting paper. After measuring a wet weight of hollow fiber membranes, membranes were allowed to dry in an oven around 60 °C for 5–6 h and dry weight (W_d) of the membranes was noted [42]. Percentage of water uptake for individual hollow fiber membranes was calculated using Eq. (6).

$$\text{Water uptake}\ (\%) = \frac{W_w - W_d}{W_w} \times 100 \tag{6}$$

The porosity of the hollow fiber membranes was investigated using dry-wet weight method [34]. The hollow fiber membranes were dipped in the distilled water for 24 h and wet weight (W_w) of the membranes was noted after the membranes were thoroughly cleaned with blotting paper. Thereafter, the membranes were dried in an air-circulating oven for overnight at 70 °C. The weight of the membranes was noted as dry weight (W_d). By using Eq. (7) the porosity of the membranes was calculated.

$$\text{P}\ (\%) = \frac{W_w - \text{W}_\text{d}}{\rho_\text{w} \times \text{A} \times \delta} \times 100 \tag{7}$$

where, 'A' is an area of the wet state of the membrane, 'δ' is hollow fiber membrane thickness and 'ρ_w' is pure water density (0.998 g/cm^3).

2.2.6. Molecular weight cut off study

A 1 wt% of polyethylene glycol (PEG) of different molecular weights 6000, 10,000 and 20,000 g/mol was used for investigation of molecular weight cut off of the prepared hollow fiber membrane. A 500 ppm of PEG (i.e. 0.5 g/L) with different molecular weight solutions was prepared using ultrapure water. The PEG rejection study was performed in a cross-flow filtration system at 1.5 bar transmembrane pressure. The same working procedure was used for filtration of PEG with the different molecular weight. In this study, initially, the feed from different

PEG solution was prepared and later PEG solution was allowed to pass through the hollow fiber membrane for filtration [43]. The concentration of PEG in the measured permeate and feed samples were determined using total organic carbon Shimadzu total organic carbon-5050A instrument [34]. Finally, the percentage rejection of PEG was measured by the Eq. (8). The interpretation, of molecular weight cut off value for the ultrafiltration process, is ranging from 1 kDa to 100 kDa.

$$\%R = 1 - \frac{C_P}{C_f} \times 100 \tag{8}$$

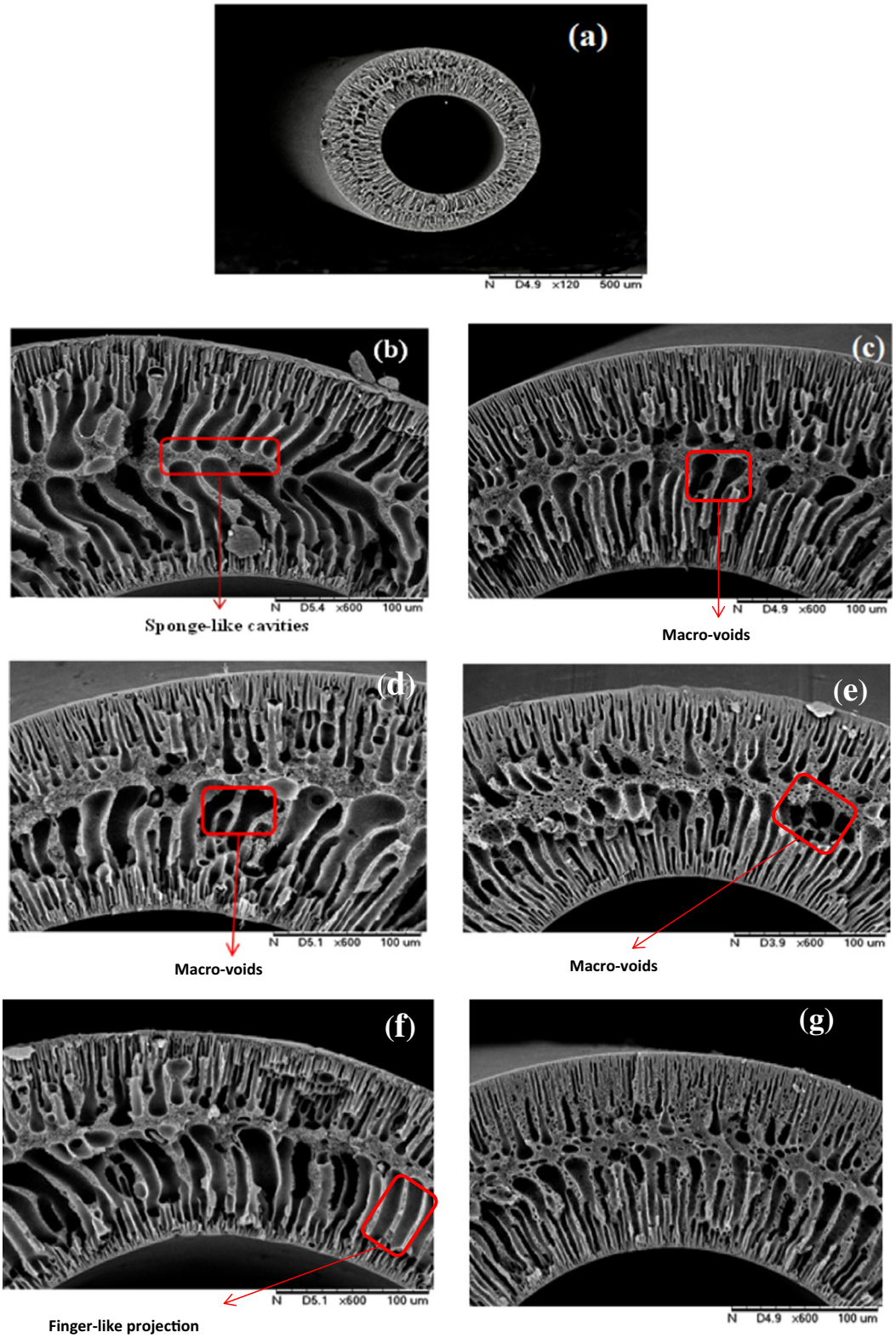

Fig. 1. SEM cross-sectional morphologies of prepared (a) neat membrane (NM) with magnification of 500 μm and followed by CA/PPSU with increased concentration of CA (b, d, and f) as CA-1, CA-3, CA-5 and CAP/PPSU with increased concentration of CAP (c, e, and g) as CAP-1, CAP-3, CAP-5 with magnification of 100 μm.

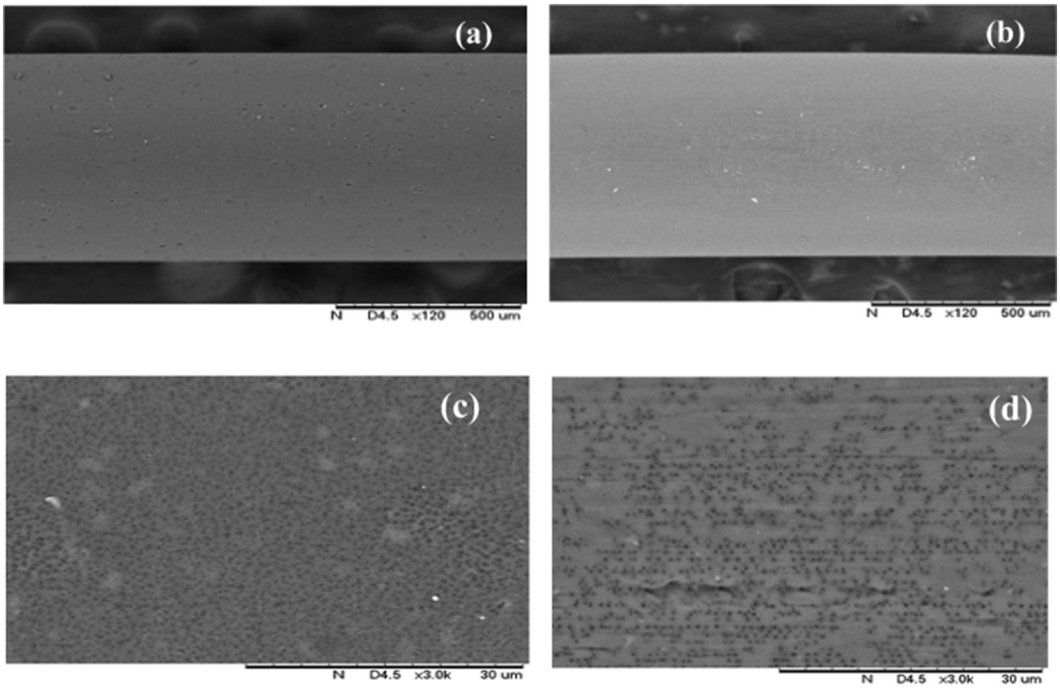

Fig. 2. SEM surface morphologies of CA-5 membrane as (a and c) with the magnification of 30 μm and CAP-5 membrane as (b and d) with the magnification of 500 μm.

where, '*R*' is solute rejection in percentage, 'C_p' is permeate flux and 'C_f' is feed of the solution.

2.2.7. The surface roughness of hollow fiber membranes

Impressions of surface roughness of the prepared -hollow fiber membranes were analyzed using atomic force microscopy (AFM) (Bruker). Hollow fiber membrane samples were cut into small pieces of the size of area 0.25 cm^2 and membranes were attached to a glass plate of area 0.50 cm^2 with the help of two-sided tape. With the aid of the tapping tool in atomic force microscopy, the prepared CA/PPSU and CAP/PPSU hollow fiber membranes were characterized by a size range of 3 × 3 μm [42,46].

2.2.8. Fourier transform infrared spectroscopy

Neat membrane, CA-5, and CAP-5 hollow fiber membranes were dried for 24 h at 60 °C to completely remove moisture from the hollow fiber membrane surfaces. Various chemical functional groups present on membrane surfaces were identified using attenuated total reflectance-fourier transform infrared (ATR-FTIR) spectroscopy from the Bruker alpha instrument. ATR-FTIR spectra of the membranes were taken in the wavelength between 4000 and 600 cm^{-1} with a 24 scan cm^{-1} [44,45].

2.2.9. The surface charge of hollow fiber membrane

The surface charge of the modified membrane (CAP-5) was determined by using the SZ-100 HORIBA nanoparticle analyzer. Membrane surface charge characterization was carried out on the surfaces of the membranes using the streaming current method with an electrokinetic SurPASS analyzer (Anton Paar GmbH, Austria). Membrane sample of 5 mg was spread in distilled water and deposited in cells of zeta potential analyzer. A 0.001 M of NaCl solvent was circulated on the measuring cell containing a sample to be measured. The prepared hollow fiber membranes were placed on the adjustable gap of area 2 × 1 cm (2 cm^2) [34,47]. Manual titrations with 0.1 M HCl and 0.1 M NaOH were done to contemplate the pH-dependent of zeta potential. The zeta potential graph of the best performance CAP-5 membrane was plotted to analyze, the surface charge of the hollow fiber membrane.

2.2.10. Study on arsenic removal from hollow fiber membranes

The percentage arsenic removal from prepared neat and blended polymeric hollow fiber membranes was evaluated using atomic absorption spectroscopy (AAS). In this study, arsenic contaminated water solution was prepared using 1 ppm arsenic. The pH of the arsenic contaminated solution was maintained at 6.8 ± 0.4. Feed of the contaminated solution was collected and noted as (C_f). Permeate was collected and the permeate flux was noted as (C_p), after passing the contaminated solution through hollow fiber membranes in a cross-flow filtration system, at 1 bar transmembrane pressure at room temperature for 60 min duration. The efficiency of arsenic rejection can be obtained by substituting AAS value of feed and permeate in Eq. (8).

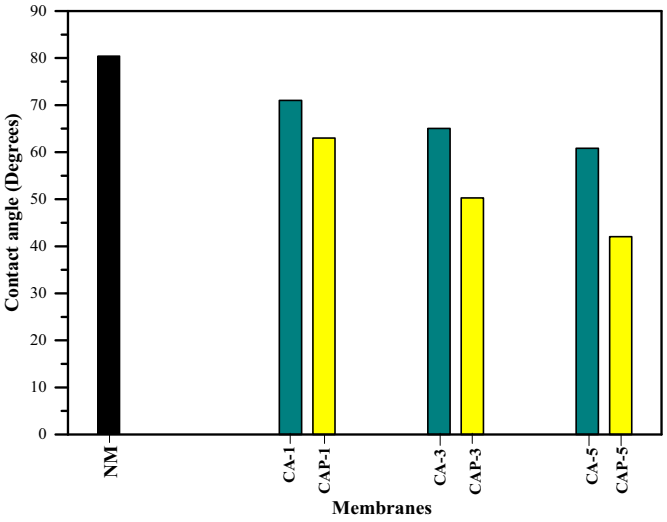

Fig. 3. Contact angle measurement for neat membrane (NM), followed by CA/PPSU with increased concentration of CA as CA-1, CA-3 and CA-5, and CAP/PPSU with increased concentration of CAP as CAP-1, CAP-3 and CAP-5.

Table 3
Properties of prepared hollow fiber membranes.

Membrane	Contact angle (°)	Porosity (%)	Water uptake (%)	Permeability (L/m^2h bar)
NM	80.48	5.48	37.50	37.92
CA-1	71.02	11.30	40.57	41.42
CA-3	65.04	19.48	55.22	48.60
CA-5	60.83	26.97	69.01	61.47
CAP-1	63.01	12.08	41.01	45.75
CAP-3	50.27	20.64	57.26	55.53
CAP-5	43.40	27.96	77.01	69.60

3. Results and discussion

3.1. Surface morphologies of the prepared hollow fiber membranes

The SEM images of CA and CAP with different concentrations in PPSU –hollow fiber membranes are shown in Figs. 1 and 2. The air gap distance between the coagulant bath and the spinneret plays an important role, in this region, the formation of hollow fiber membranes takes place [48]. Smaller air gap results in more finger-like structures [27]. From Fig. 1a, it is clear that the neat membrane does not produce finger-like morphological structures. Neat membrane intern produces a porous like structure as a result of interaction between water and solvent in the coagulation bath. Finger -like and sponge -like morphological structures are evidenced with increased percentages of additives (CA and CAP) in the casting solution (1, 3 and 5 wt%) was shown in Fig. 1(b–g) which results in enhancing permeability, water uptake and porosity of prepared hollow fiber membranes during filtration processes. Furthermore, the increase in water permeability of hollow fiber membrane can be observed due to the presence of horizontal channels present in the membrane microstructure [49]. With the increase in CAP additives, extreme pore structures can be observed (Fig. 1g) as compared to CA along with PPSU –hollow fiber membranes (Fig. 1e). However, this causes an increase in the percentage rejection of arsenic contaminated water from CAP/PPSU –hollow fiber membranes. A large number of voids can be observed from the CAP-5 hollow fiber membrane. Beyond this highest value, the hollow fiber membranes are not suitable for any separation processes.

3.2. Hydrophilicity of the prepared hollow fiber membranes

Contact angle measurements for pristine and blend hollow fiber membranes were investigated to evaluate the properties such as hydrophilicity and hydrophobicity. The experimental results from Fig. 3 indicated an increase in hydrophilicity with an incremental dosage of CA and CAP in PPSU dope solutions. From Table 3 neat membrane (without adding additives) exhibited the higher value of contact angle as 80.48^0 and further addition of additives the contact angle value decreases considerably, with the increased addition of CA and CAP in PPSU was CA-5 as 60.83° and CAP-5 as 43.40° respectively. The presence of carboxyl and hydroxyl groups on CAP membrane surfaces helps in absorption of water molecules, which results in the enhancement of

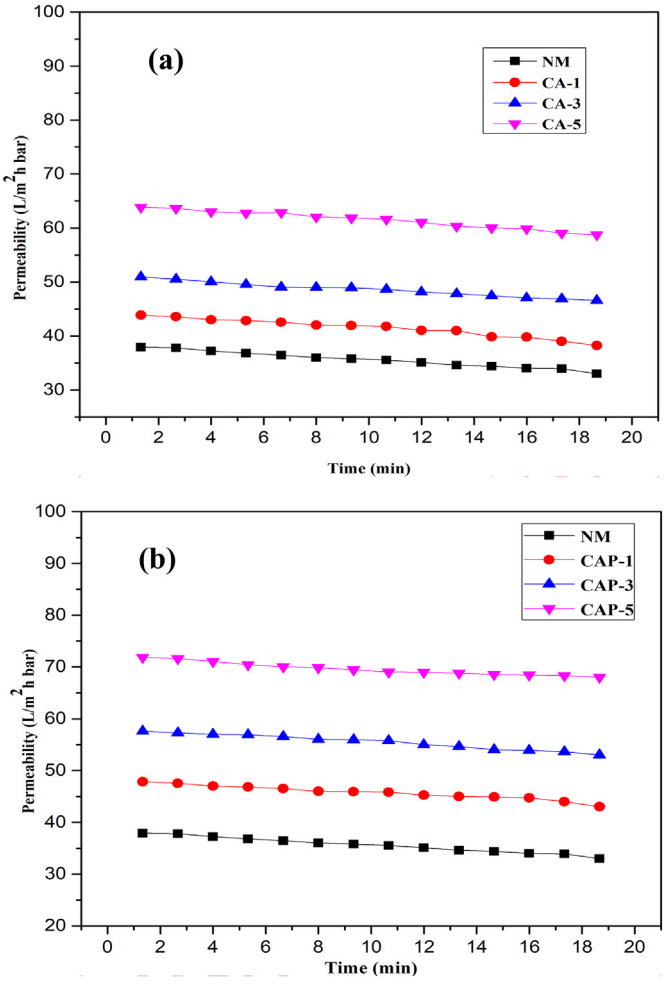

Fig. 4. (a) Time-dependent pure water permeability for neat membrane (NM), CA/PPSU with increased concentration of CA as CA-1, CA-3 and CA-5, and (b) CAP/PPSU with increased concentration of CAP as CAP-1, CAP-3 and CAP-5 with an operating pressure of 1 bar at room temperature.

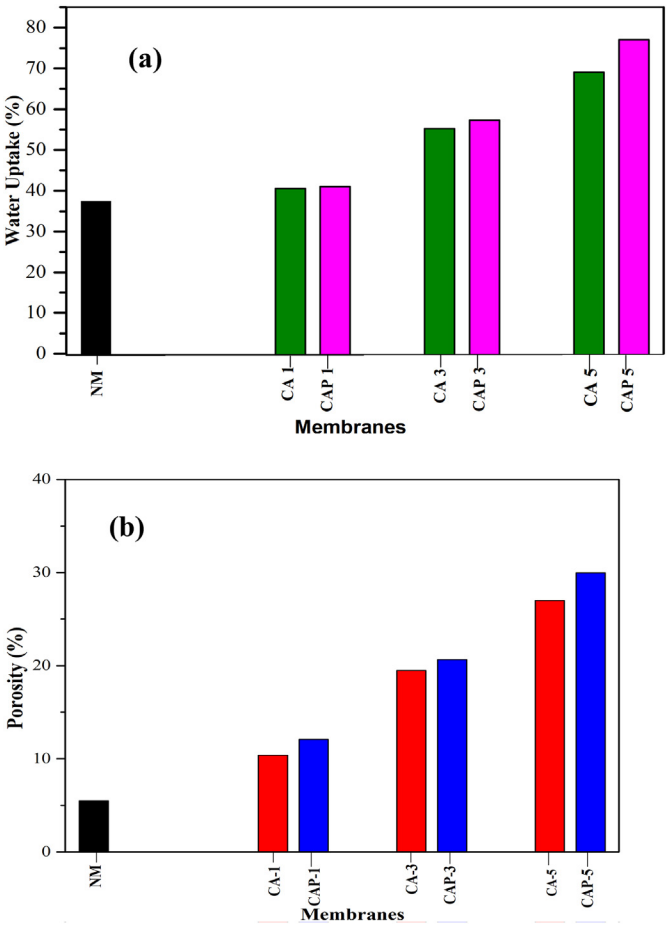

Fig. 5. (a) Water uptake and (b) Porosity measurement, for neat membrane (NM), followed by CA/PPSU with increased concentration of CA as CA-1, CA-3 and CA-5, and CAP/PPSU with increased concentration of CAP as CAP-1, CAP-3 and CAP-5.

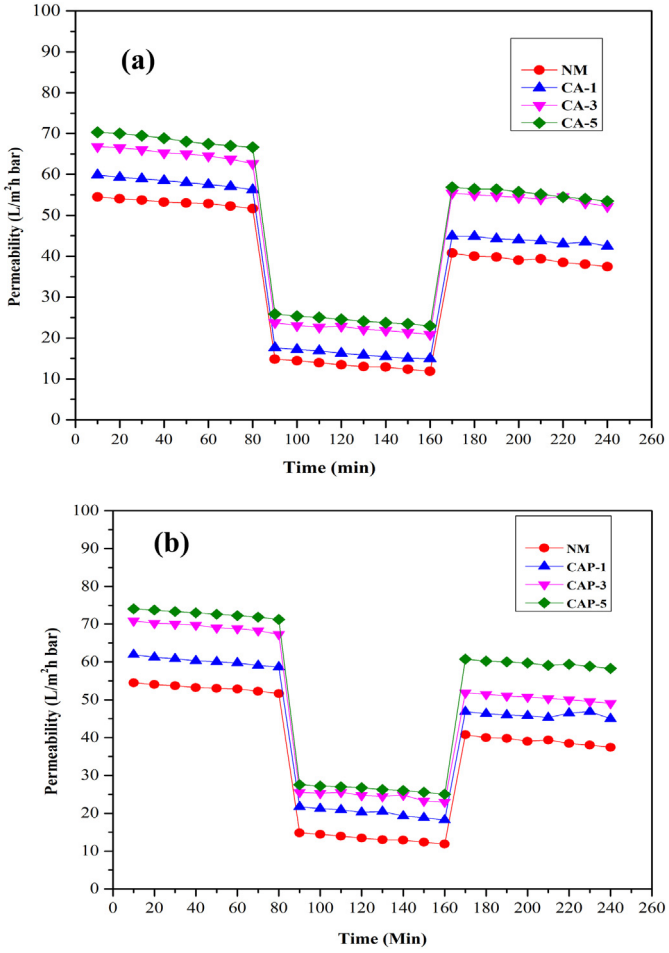

Fig. 6. Time dependant pure water permeability, protein BSA permeability, and pure water permeability after washing with water for (a) neat membrane (NM), CA/PPSU with increased concentration of CA as CA-1, CA-3 and CA-5, and (b) neat membrane (NM), CAP/PPSU with increased concentration of CAP as CAP-1, CAP-3 and CAP-5 with operating pressure of 1 bar at room temperature.

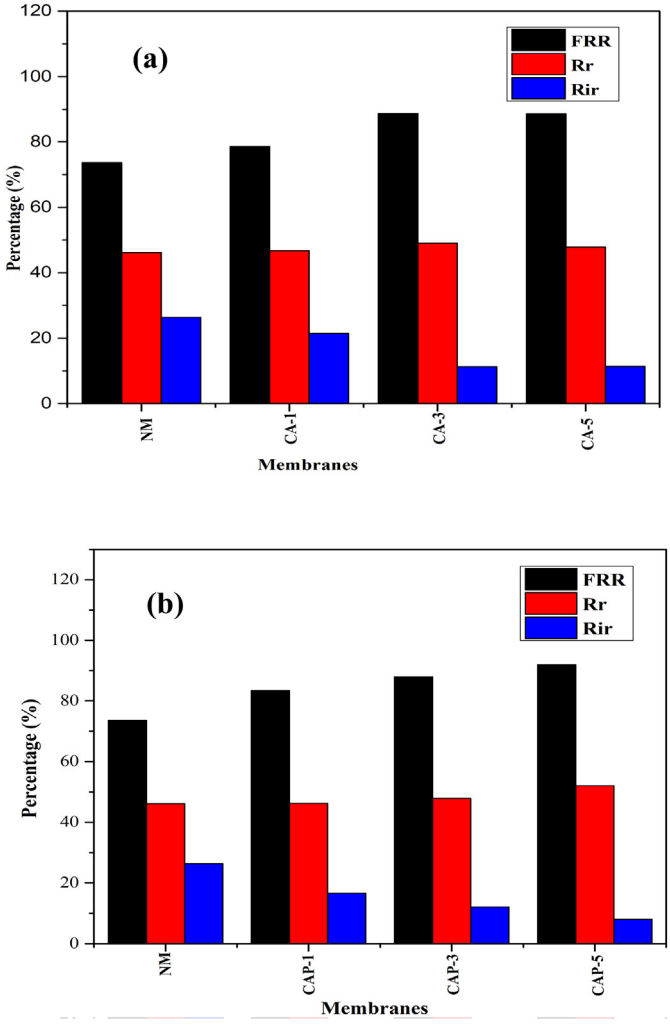

Fig. 7. Flux recovery ratio (FRR), reversible fouling (R_r) and irreversible fouling (R_{ir}) values for (a) neat membrane (NM), CA/PPSU with increased concentration of CA as CA-1, CA-3 and CA-5, and (b) neat membrane (NM), CAP/PPSU with increased concentration of CAP as CAP-1, CAP-3 and CAP-5.

hydrophilicity on membrane surfaces. The decreased value of the contact angle measured by the instrument for CAP hollow fiber membranes is shown as CAP-0 < CAP-1 < CAP-3 < CAP-5. The effect of increased proportions of CA -hollow fiber membranes with a decrease in the value of contact angle is given by CA-0 < CA-1 < CA-3 < CA-5.

3.3. Pure water permeability study of hollow fiber membranes

Hydrophilicity, and porosity, are the main governing factors for studying the flux of prepared hollow fiber membranes [50]. Pure water permeability in terms of the time-dependent study was performed using a cross-flow filtration system at 0.3 MPa transmembrane pressure. The variation of pure water permeability for different kinds of membranes is reported in Table 3. Generally, the pure water permeability of the membrane has a direct co-relation with an average pore size and porosity of the membrane. From Table 3, the value of pure water permeability for

Table 4
Antifouling properties of the prepared hollow fiber membranes.

Membrane sample	J_{w1} (L/m² h bar)	J_{w2} (L/m² h bar)	J_p (L/m² h bar)	FRR (%)	R_r (%)	R_{ir} (%)	R_t (%)
NM	48.52	35.73	13.34	73.64	46.15	26.36	72.51
CA-1	50.71	39.85	16.15	78.58	46.73	21.41	67.15
CA-3	56.25	49.89	22.30	88.70	49.05	11.30	60.35
CA-5	64.63	57.31	26.38	88.67	47.85	11.32	59.18
CAP-1	54.25	45.21	20.12	88.33	46.24	16.66	62.19
CAP-3	61.32	53.91	24.58	87.91	47.83	12.08	59.91
CAP-5	71.26	65.52	28.41	91.95	52.08	8.06	60.13

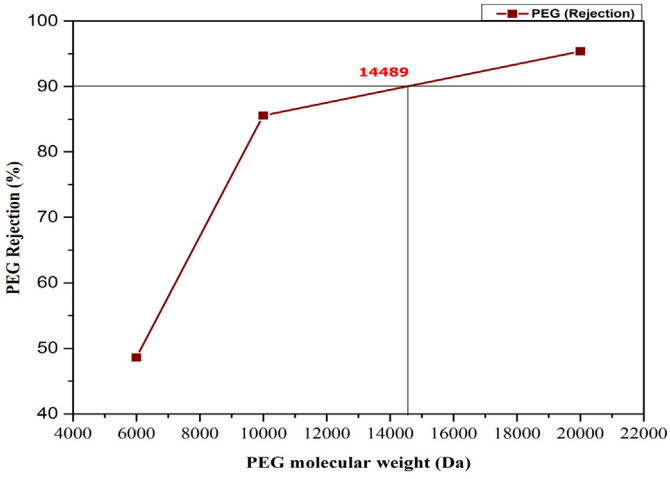

Fig. 8. Molecular weight cutoff studies of CAP-5 hollow fiber membrane with rejection transmembrane pressure of 1 bar at room temperature.

neat hollow fiber membrane as 37.92 L/m^{2}h bar, CA-5 membrane as 61.47 L/m^{2}h bar and CAP-5 membrane as 69.60 L/m^{2}h bar respectively. There is a significant change in the permeation performance of hollow fiber membranes after the addition of the increased percentages of additives (CA and CAP) to PPSU dope solution. This is because of the amorphous nature of CA and CAP additive causes an increase in porosity

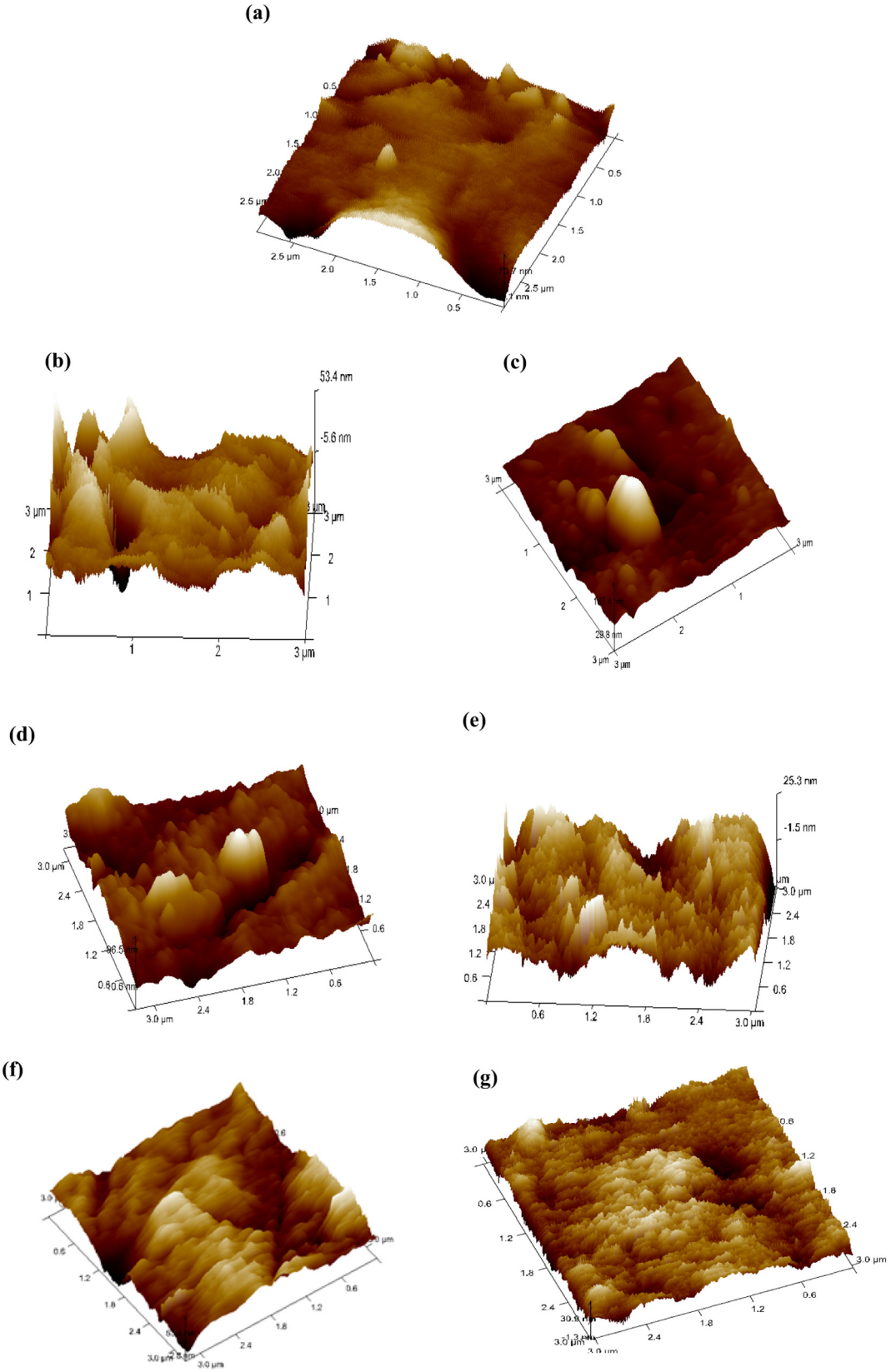

Fig. 9. Atomic force microscopy images for (a) neat membrane (NM) and followed by CA/PPSU with increased concentration of CA (b, d, and f) as CA-1, CA-3 and CAP/PPSU with increased concentration of CAP (c, e, and g) as CAP-1, CAP-3 and CAP-5.

Table 5
Surface roughness value of prepared hollow fiber membranes.

Membranes	R_a (nm)	R_q (nm)	R_z (nm)	R_{max} (nm)
NM	8.05	12	3.72	108
CA-1	9.5	13.5	4.24	160
CA-3	22.5	29.6	8.26	203
CA-5	39.8	49.9	10.30	386
CAP-1	20.1	30.6	5.14	242
CAP-3	26.3	39.3	12.53	365
CAP-5	47.4	61.4	28.35	442

in the membrane [15]. From Fig. 4a and b, the CAP-5 hollow fiber membranes, revealed increased permeation property compared to CA-5 hollow fiber membranes, because CAP is more hydrophilic in nature and has significant water holding ability which allows facile flow of water through the hollow fiber membranes.

3.4. Water uptake and porosity study

Fig. 5a and b revealed that the water uptake and porosity values increased considerably with incremental dosages of hydrophilic CA and CAP in hydrophobic PPSU. The porosity of hollow fiber membranes has a close relation with membrane performance and morphology [51]. From Fig. 5(a) and Table 3, the value of porosity for neat membrane was recorded as 5.48% and adding 5 wt% of CA and CAP into PPSU dope solution, resulted in enhancement of the porosity values as CA-5 and CAP-5 was 26.97 and 27.96%, respectively. Similarly, from Fig. 5(b) and Table 3, the value of water uptake for prepared hollow fiber membranes without additives was 37.50%. It was observed that, the increased concentrated additive membranes CA-5 and CAP-5 resulted in increased water uptake value as 69.01 and 77.01%, respectively. Increased value of water uptake and porosity was observed from CAP hollow fiber membranes, due to more water holding capacity of the CAP additive as compared to CA additive present in the hollow fiber membranes. Another reason for the enhancement of porosity and water uptake is that, the addition of the increased percentage of additives leads to thermal instability, which causes rapid de-mixing in the coagulation bath [52]. The considerable increase in the value of water uptake and porosity results are CA-0 < CA-1 < CA-3 < CA-5 and same as CAP-0 < CAP-1 < CAP-3 < CAP-5.

3.5. Antifouling properties of hollow fiber membranes

Fig. 6(a) and (b) demonstrated an enhanced BSA permeability study. By incremental dosage of hydrophilic additives (CA and CAP), there was an increase in the permeability, which was due to the adsorptive nature of both the additives. From Table 4, the value of flux recovery ratio (FRR) for neat membrane was 73.64% and the total recovery ratio (R_t) was 72.51%. With the addition of 5 wt% of CA (CA-5) in the PPSU casting solution, there is an increase in the value of FRR as 88.67%, 5 wt% of CAP (CAP-5) was 91.95% and decrease in R_t value as 72.51% for neat membrane to 59.18 and 60.13% for CA-5 and CAP-5 respectively was noticed from Fig.6a and b. An increased value of FRR promises the better antifouling property for CAP as compared to the neat and CA membrane. This is due to the presence of an enormous amount of hydroxyl

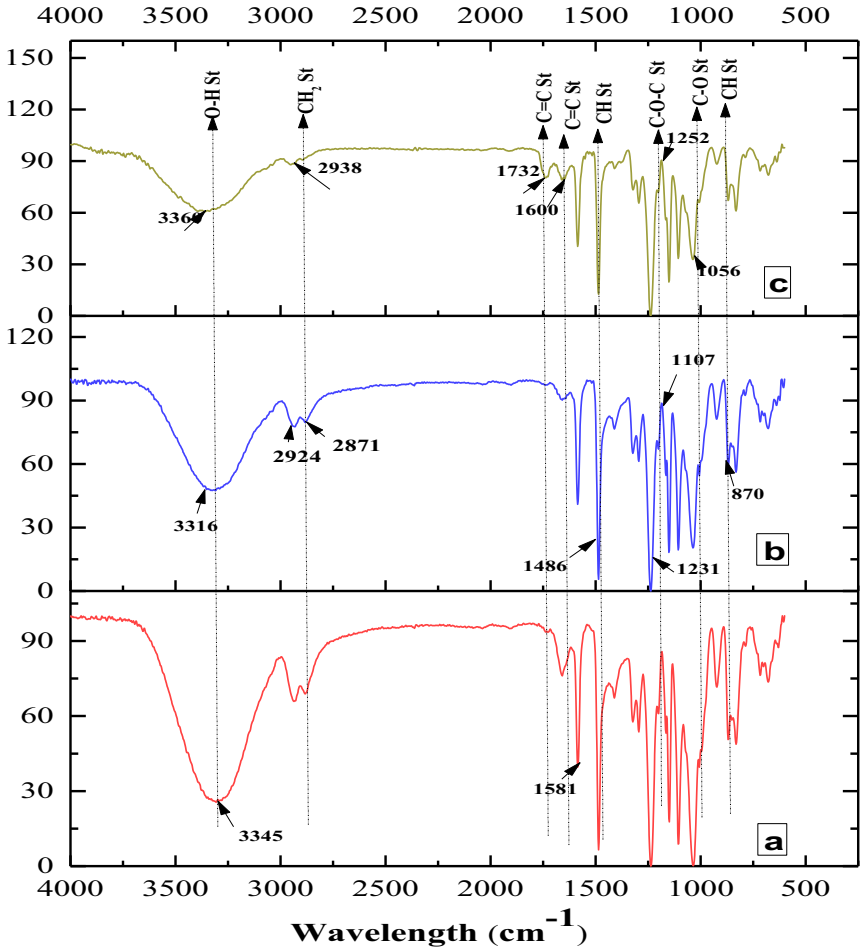

Fig. 10. ATR-FTIR spectra for (a) Neat membrane (NM), (b) CA-5 and (c) CAP-5 hollow fiber membranes.

and amine groups on the surfaces of the CAP hollow fiber membranes which further leads to an increase in hydrophilicity [53]. In BSA fouling study, protein molecules were deposited on the surfaces of hollow fiber membranes, which results in a decline of permeability due to pore blockage. The reversible (R_r) and irreversible (R_{ir}) hydraulic fouling are two main membrane fouling categories. From Table 4, the value of R_r for neat membrane was 46.15% with enhanced additive concentrated membrane CA-5 and CAP-5 was 47.85 and 52.08%, respectively. This indicated that, the blended hollow fiber membranes exhibited an increased value of R_r, and FRR. From Fig. 7a and b, the decreased value of R_{ir} from the neat membrane (26.36%) and increased percentage of additive membranes as CA-5 was 11.32% and CAP-5 was 8.06%, ensured the good filtration life of blended membranes.

3.6. Molecular weight cut-off

From Fig. 8, the molecular weight cut-off (MWCO) value for best performance membrane CAP-5 was 14,489 Da, which revealed that as prepared hollow fiber membrane was ultrafiltration membrane [54]. The CAP-5 hollow fiber membrane revealed the rejection of 47, 85 and 94% for polyethylene glycol (PEG) 6000, 10,000 and 20,000, respectively. As the molecular weight of the PEG increased the rejection percentage of the PEG from prepared hollow fiber membranes is also increased [55,56].

3.7. The surface roughness of hollow fiber membranes

Fig. 9 illustrated 3D AFM topological images of the neat hollow fiber membrane, CA/PPSU and CAP/PPSU blended hollow fiber membranes. The study of handling the tapping mode AFM apparatus was explained elsewhere [57]. Generally, surface roughness value mainly depends on the arithmetic mean deviation of roughness (R_a), root mean square Z- data (R_q) and the height difference between five maximum height peaks and five minimum height peaks (R_z) [46]. Commonly, the value of the surface roughness (Ra) will be considered to scrutinize the nature of roughness. From Table 5, neat membrane (NM) shows R_a value as 8.05 nm which is without the addition of additives (CA and CAP). Further, increased additive concentrated membranes, CA-5 and CAP-5 shows R_a value as 39.8 nm 47.4 nm, respectively. The CAP-5 hollow fiber membrane consists of increased surface roughness is evidenced from Fig. 9g, which reduces the tendency towards fouling and leads to an increase in arsenic rejection efficacy [58]. However, in case of CA -hollow fiber membranes (Fig. 9f), lower values of average roughness (R_a) contain fewer pores on the surface which leads to decrease in the percentage of arsenic rejection by hollow fiber membranes [59].

3.8. Fourier transform infrared (FT-IR) spectroscopy

Fig. 10 shows the ATR-FTIR spectra, which clearly represents the changes in functional groups due to the presence of CA and CAP additives, as compared to the neat membrane as shown in Fig. 10a. All absorption peaks attributed less than 2000 cm^{-1} of wavelength range. FTIR of CA shows (Fig.10b) the peaks at 3316 cm^{-1} which attributed to the stretching vibration of –OH group. CAP shows (Fig. 10c) a peak of –OH group at 3360 cm^{-1}, this is due to the presence of hydroxyl group. The peaks 2924–2871 cm^{-1} attributed to $-CH_2$ stretching vibration present in the CA. The alkyl group was characterized by a peak present at 1486 cm^{-1}, peak observed at 1231 cm^{-1} indicates stretching vibration bond corresponds to a cyclic ether group of CA. Similarly, the C-O-C stretching vibration was observed at 1107 cm^{-1} and peak found at 870 cm^{-1} attributed to –CH group of CA [60–62]. Whereas in the pure CAP, 3360–2938 cm^{-1} attributed to symmetric stretching of cellulose –C-H– group, 1056 cm^{-1} –C-O- stretching vibration, 1252 cm^{-1} –C-O- C- stretching vibration, 1600 cm^{-1} -C=C- attributed to a conjugated vinyl aromatic ring, 1732 cm^{-1} represents

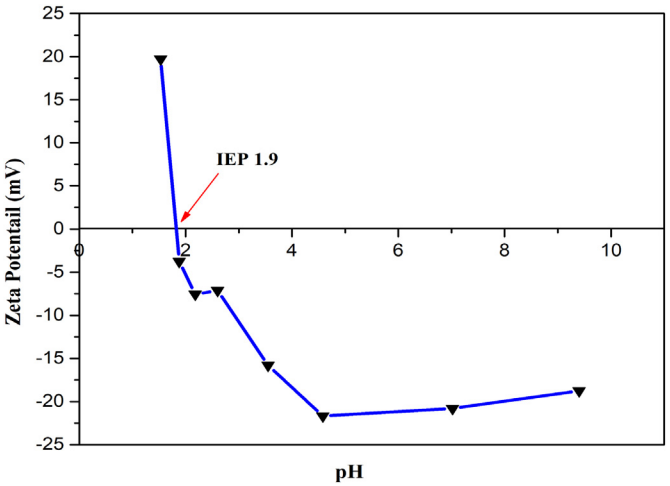

Fig. 11. Surface charge (Zeta potential) studies of CAP-5 hollow fiber membrane as a function of pH.

–C=C- a carboxylic group [62,63]. The carboxylic peak of 1732 cm^{-1} was not present in the neat membrane as compared to CA and CAP hollow fiber membranes [64,65]. The FT-IR peaks confirm the presence of CA and CAP additives in PPSU membrane matrix.

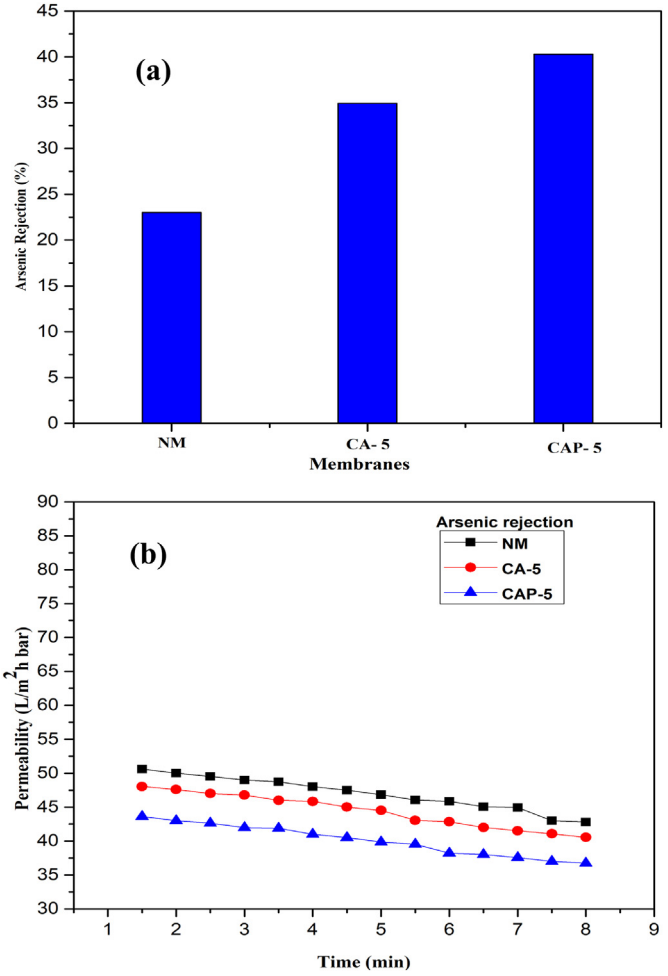

Fig. 12. (a) Comparison of arsenic rejection in percentage (b) Time-dependent permeability for arsenic rejection study of the prepared neat membrane (NM), CA-5 and CAP-5 hollow fiber membranes with transmembrane pressure of 1 bar at room temperature.

Table 6
Arsenic removal from used polymer (PPSU) and additives (CA and CAP) membranes.

Membrane composition	Arsenic feed	Flux (L/m^{2}h bar)	Rejection (%)	Reference
Cellulose acetate (CA)/zinc oxide	1000 mg/litre	18.41	58.77	[72]
Cellulose triacetate (CTA)/activated carbon (AC))	500 ppb	5.23	45.00	[18]
CA poly-isophthalamide-*graft*-methacrylamide (CA/PIPA-g-MAA)-polyetherimine (PEI)	100ppm	28.86	83.80	[19]
Polyphenylsulfone (PPSU)/carboxylated graphene oxide (GO)	10 ppm	2.88	~99.00	[68]
Cellulose triacetate (CTA) and propionate lignin	–	0.19	26.32	[3]
Cellulose acetate/polyphenylsulfone and cellulose acetate phthalate/polyphenylsulfone	1 ppm	61.47 (CA/PPSU)	34	Present work
		69.60 (CAP/PPSU)	41	

3.9. Surface charge measurement of hollow fiber membrane

Fig. 11 shows the zeta potential of membrane CAP-5, as pH on the x-axis and the values of zeta potential as on the y-axis of the prepared CAP-5/PPSU hollow fiber membrane. The pH value of this study was adjusted between pH 1.5 to 9.7 with the addition of 0.1 N HCl and KOH. Zeta potential characterization is an effective technique for finding the surface charge of the prepared membrane [66]. However, the acquired results can be summarized as surfaces of the membranes are positively charged over the range of pH 1.53 and negatively charged over a range of pH 9.7. The highest zeta potential −18.75 mV was recorded corresponding to pH 9.7 [66,67]. Due to the implementation of CAP as an additive and at these pH levels, ions of arsenic were repelled. The pH at 1.9 represents the isoelectric point (IEP) of the membrane, at this pH surface charge becomes zero and membrane surfaces are not subjected to any surface charge. The surface of blended PPSU/CAP hollow fiber membrane was charged negatively because of the presence of carboxylated groups.

3.10. Study on the removal of arsenic from prepared hollow fiber membranes

Fig. 12 shows the comparison of arsenic rejection on the neat membrane, CA-5 and CAP-5 hollow fiber membranes. The blended CA and CAP hollow fiber membranes were tested for rejection of arsenic prepared from laboratory aqueous solution (1 ppm of arsenic). The used CA and CAP additives have good adsorptive properties for arsenic removal [69]. The CAP membranes showed the considerable removal of arsenic (41% for CAP-5) as compared to the neat membrane (22%) and CA membranes (34% for CA-5), because CAP hollow fiber membranes contain higher adsorptive property and moreover, less tendency towards fouling and higher permeability [63]. The rejection phenomenon of hollow fiber membranes also depends on the molecular weight of the additives used. The molecular weight of the CAP was higher than CA membrane which influences the enhanced removal of arsenic over CA membranes. Fig. 12b shows time-dependent pure water permeability studies for arsenic removal of neat, CA-5 and CAP-5 hollow fiber membranes. The permeability value for arsenic removal from neat membrane was 47 L/m^{2}h bar, CA-5 was 44.42 L/m^{2}h bar and CAP-5 was 40.11 L/m^{2}h bar. Initially, the rejection of the arsenic was higher and further there was a gradual decline was observed, which is due to the fouling behavior of the membrane. The ions of arsenic were deposited on the membrane surfaces which intern block the pores which resulted in lowering the rejection permeability and enhancing the rejection percentage of arsenic. In addition to this, concentration polarization is also the main reason for the decline of arsenic removal permeability [70]. From Fig. 12a, CAP-5 rejected increased arsenic contamination from water because of higher adsorptive nature. Thus, CAP-5 membrane considered as the best performance membrane based on its higher hydrophilicity, porosity, water uptake and less fouling tendency [71]. Furthermore, details for arsenic removal from the literature was illustrated in Table 6 describes the comparison of already reported hollow fiber membranes and present hollow fiber membranes for percentage removal of arsenic with respect to used polymer (polyphenylsulfone) and additive (cellulose acetate).

4. Conclusion

Cellulose acetate, cellulose acetate phthalate and polyphenylsulfone asymmetric hollow fiber membranes were prepared using a dry-wet phase inversion technique. The incremental dosage of hydrophilic additives resulted in more finger-like projections and micro-voids which help in the enhancement of permeability as compared to the pristine membrane. Removal of arsenic from contaminated ground-water mainly depends on pH in the range of 1.5 to 9.7 for CAP-5 hollow fiber membrane. The molecular weight cutoff was 14,485 Da for CAP-5, which indicated as fabricated membranes are ultrafiltration membranes. AFM results revealed an increase in surface roughness of hollow fiber membranes due to an increased concentration of additives into the polyphenylsulfone matrix. The CAP-5 hollow fiber membrane considered as best performance membrane due it's increased properties such as higher hydrophilicity, less tendency towards fouling, higher water uptake and increased overall porosity. Arsenic removal was found to be 34% for CA-5 membrane and 41% for CAP-5 membrane, respectively. In conclusion, prepared cellulose acetate/polyphenylsulfone and cellulose acetate phthalate/polyphenylsulfone hollow fiber ultrafiltration membranes are ideal candidates for the preliminary removal of the arsenic present in the water bodies.

Acknowledgements

Authors acknowledge the Director, NITK Surathkal, India for furnishing the research facilities. Authors greatfully express thanks to University Technology Malaysia (UTM) Malaysia for providing outstanding research facilities and collaboration of research. Authors thankful to Head, Dept. of Chemical Engineering, NITK Surathkal for providing the total organic carbon (TOC) analysis.

References

[1] N. Varma, I. Singh, M.S. Dahiya, V.K. Ravi, S. Kumar, Structural perturbation by arsenic triggers the aggregation of hen egg white lysozyme by promoting oligomers formation, Int. J. Biol. Macromol. 109 (2018) 1108–1114.
[2] N. Pandey, R. Bhatt, Improved biotransformation of arsenic by arsenite oxidase—chitosan nanoparticle conjugates, Int. J. Biol. Macromol. 106 (2018) 258–265.
[3] L.M. Nevárez, L.B. Casarrubias, O.S. Canto, A. Celzard, V. Fierro, R.I. Gómez, G.G. Sánchez, Biopolymers-based nanocomposites: membranes from propionated lignin and cellulose for water purification, Carbohydr. Polym. 86 (2011) 732–741.
[4] Z. Zhou, Y. Liu, S. Liu, H. Liu, G. Zeng, X. Tan, C. Yang, Y. Ding, Z. Yan, X. Cai, Sorption performance and mechanisms of arsenic (V) removal by magnetic gelatin-modified biochar, Chem. Eng. J. 314 (2017) 223–231.
[5] J. Wang, W. Xu, L. Chen, X. Huang, J. Liu, Preparation and evaluation of magnetic nanoparticles impregnated chitosan beads for arsenic removal from water, Chem. Eng. J. 251 (2014) 25–34.
[6] M. Yüksel, Ü. Yükel, S.A. Tuncel, K. Yoshizuka, M. Bryjak, S. Samatya, P.K. Yilmaz, İ.Y. Ipek, N. Kabay, Removal of boron and arsenic from geothermal water by ion-exchange, Geotherm. Water Manag, CRC Press 2018, pp. 135–155.
[7] G.L. Ghurye, D.A. Clifford, A.R. Tripp, Combined arsenic and nitrate removal by ion exchange, J. Am. Water Works Assoc. 91 (1999) 85–96.

[8] C.J. Srinivasakannan, Arsenic Removal through Electro Coagulation: Kinetics and Statistical Modelling, 2009.
[9] L. Hao, N. Wang, C. Wang, G. Li, Arsenic removal from water and river water by the combined adsorption-UF membrane process, Chemosphere 202 (2018) 768–776.
[10] A. Abejón, A. Garea, A. Irabien, Arsenic removal from drinking water by reverse osmosis: minimization of costs and energy consumption, Sep. Purif. Technol. 144 (2015) 46–53.
[11] R. Rezaee, S. Nasseri, A.H. Mahvi, R. Nabizadeh, S.A. Mousavi, A. Rashidi, A. Jafari, S. Nazmara, Fabrication and characterization of a polysulfone-graphene oxide nanocomposite membrane for arsenate rejection from water, J. Environ. Health Sci. Eng. 13 (2015) 61.
[12] J. He, T. Matsuura, J.P. Chen, A novel Zr-based nanoparticle-embedded PSf blend hollow fiber membrane for treatment of arsenate contaminated water: material development, adsorption and filtration studies, and characterization, J. Membr. Sci. 452 (2014) 433–445.
[13] R.J. Gohari, W.J. Lau, T. Matsuura, A.F. Ismail, Fabrication and characterization of novel PES/Fe–Mn binary oxide UF mixed matrix membrane for adsorptive removal of As (III) from contaminated water solution, Sep. Purif. Technol. 118 (2013) 64–72.
[14] J. Song, M. Zhang, A. Figoli, Y. Yin, B. Zhao, X.-M. Li, T. He, Arsenic removal using a sulfonated poly (ether ether ketone) coated hollow fiber nanofiltration membrane, Environ. Sci.: Water Res. Technol. 1 (2015) 839–845.
[15] S. Chatterjee, S. De, Adsorptive removal of arsenic from groundwater using a novel high flux polyacrylonitrile (PAN)–laterite mixed matrix ultrafiltration membrane, Environ. Sci.: Water Res. Technol. 1 (2015) 227–243.
[16] M. Khayet, K.C. Khulbe, T. Matsuura, Characterization of membranes for membrane distillation by atomic force microscopy and estimation of their water vapor transfer coefficients in vacuum membrane distillation process, J. Membr. Sci. 238 (2004) 199–211.
[17] X. He, Fabrication of defect-free cellulose acetate hollow fibers by optimization of spinning parameters, Membranes 7 (2017) 27.
[18] L.P. Terrazas-Bandala, G. Gonzalez-Sanchez, R. Garcia-Valls, T. Gumi, I. Beurroies, R. Denoyel, C. Torras, L. Ballinas-Casarrubias, Influence of humidity, temperature, and the addition of activated carbon on the preparation of cellulose acetate membranes and their ability to remove arsenic from water, J. Appl. Polym. Sci. 131 (n.d.). doi: https://doi.org/10.1002/app.40134.
[19] A. Jayalakshmi, S. Rajesh, S. Senthilkumar, H.H. Sankar, D. Mohan, Preparation of poly (isophthalamide-graft-methacrylamide) and its utilization in the modification of cellulose acetate ultrafiltration membranes, J. Ind. Eng. Chem. 20 (2014) 133–144.
[20] D.K. Bhat, H.S. Jois, Miscibility and conductivity studies of poly (methyl methacrylate) and cellulose acetate phthalate blends, Procedia Mater. Sci. 5 (2014) 995–1004.
[21] A. Seidel, J.J. Waypa, M. Elimelech, Role of charge (Donnan) exclusion in removal of arsenic from water by a negatively charged porous nanofiltration membrane, Environ. Eng. Sci. 18 (2001) 105–113.
[22] M. Rezakazemi, M. Sadrzadeh, T. Matsuura, Thermally stable polymers for advanced high-performance gas separation membranes, Prog. Energy Combust. Sci. 66 (2018) 1–41.
[23] M. Rezakazemi, A. Khajeh, M. Mesbah, Membrane filtration of wastewater from gas and oil production, Environ. Chem. Lett. (2018) 1–22.
[24] M. Rezakazemi, A. Dashti, H.R. Harami, N. Hajilari, Fouling-resistant membranes for water reuse, Environ. Chem. Lett. (2018) 1–49.
[25] S. Vetrivel, M.S.A. Saraswathi, D. Rana, K. Divya, A. Nagendran, Cellulose acetate composite membranes tailored with exfoliated tungsten disulfide nanosheets: permeation characteristics and antifouling ability, Int. J. Biol. Macromol. 115 (2018) 540–546.
[26] S. Vetrivel, M.S.A. Saraswathi, D. Rana, A. Nagendran, Fabrication of cellulose acetate nanocomposite membranes using 2D layered nanomaterials for macromolecular separation, Int. J. Biol. Macromol. 107 (2018) 1607–1612.
[27] S. Shenvi, A.F. Ismail, A.M. Isloor, Enhanced permeation performance of cellulose acetate ultrafiltration membranes by incorporation of sulfonated poly (1, 4-phenylene ether ether sulfone) and poly (styrene-co-maleic anhydride), Ind. Eng. Chem. Res. 53 (2014) 13820–13827.
[28] S.S. Shenvi, A.M. Isloor, A.L. Ahmad, B. Garudachari, A.F. Ismail, Influence of palm oil fuel ash, an agro-industry waste on the ultrafiltration performance of cellulose acetate butyrate membrane, Desalin. Water Treat. 57 (2016) 26414–26426.
[29] M.C. Nayak, A.M. Isloor, A. Moslehyani, N. Ismail, A.F. Ismail, Fabrication of novel PPSU/ZSM-5 ultrafiltration hollow fiber membranes for separation of proteins and hazardous reactive dyes, J. Taiwan Inst. Chem. Eng. 82 (2018) 342–350.
[30] I.K. Moideen, A.M. Isloor, A.F. Ismail, A. Obaid, H.-K. Fun, Fabrication and characterization of new PSf/PPSU UF blend membrane for heavy metal rejection, Desalin. Water Treat. 57 (2016) 19810–19819.
[31] S. Darvishmanesh, J.C. Jansen, F. Tasselli, E. Tocci, P. Luis, J. Degrève, E. Drioli, B. Van der Bruggen, Novel polyphenylsulfone membrane for potential use in solvent nanofiltration, J. Membr. Sci. 379 (2011) 60–68.
[32] L. Luo, G. Han, T.-S. Chung, M. Weber, C. Staudt, C. Maletzko, Oil/water separation via ultrafiltration by novel triangle-shape tri-bore hollow fiber membranes from sulfonated polyphenylenesulfone, J. Membr. Sci. 476 (2015) 162–170.
[33] M. Golpour, M. Pakizeh, Preparation and characterization of new PA-MOF/PPSU-GO membrane for the separation of KHI from water, Chem. Eng. J. 345 (2018) 221–232.
[34] G.S. Ibrahim, A.M. Isloor, A.M. Asiri, N. Ismail, A.F. Ismail, G.M. Ashraf, Novel, one-step synthesis of zwitterionic polymer nanoparticles via distillation-precipitation polymerization and its application for dye removal membrane, Sci. Rep. 7 (2017) 15889.
[35] R.S. Hebbar, A.M. Isloor, K. Ananda, A.F. Ismail, Fabrication of polydopamine functionalized halloysite nanotube/polyetherimide membranes for heavy metal removal, J. Mater. Chem. A 4 (2016) 764–774.
[36] I.K. Moideen, A.M. Isloor, B. Garudachari, A.F. Ismail, The effect of glycine betaine additive on the PPSU/PSf ultrafiltration membrane performance, Desalin. Water Treat. 57 (2016) 24788–24798.
[37] B.M. Ganesh, A.M. Isloor, A.F. Ismail, Enhanced hydrophilicity and salt rejection study of graphene oxide-polysulfone mixed matrix membrane, Desalination 313 (2013) 199–207.
[38] R. Kumar, A.M. Isloor, A.F. Ismail, T. Matsuura, Performance improvement of polysulfone ultrafiltration membrane using N-succinyl chitosan as additive, Desalination 318 (2013) 1–8.
[39] R.S. Hebbar, A.M. Isloor, A.K. Zulhairun, M.S. Abdullah, A.F. Ismail, Efficient treatment of hazardous reactive dye effluents through antifouling polyetherimide hollow fiber membrane embedded with functionalized halloysite nanotubes, J. Taiwan Inst. Chem. Eng. 72 (2017) 244–252.
[40] R.S. Hebbar, A.M. Isloor, A.F. Ismail, S.J. Shilton, A. Obaid, H.-K. Fun, Probing the morphology and anti-organic fouling behaviour of a polyetherimide membrane modified with hydrophilic organic acids as additives, New J. Chem. 39 (2015) 6141–6150.
[41] V.R. Pereira, A.M. Isloor, A. Al Ahmed, A.F. Ismail, Preparation, characterization and the effect of PANI coated TiO_2 nanocomposites on the performance of polysulfone ultrafiltration membranes, New J. Chem. 39 (2015) 703–712.
[42] R.S. Hebbar, A.M. Isloor, B. Prabhu, Inamuddin, A.M. Asiri, A.F. Ismail, Removal of metal ions and humic acids through polyetherimide membrane with grafted bentonite clay, Sci. Rep. 8 (2018) 4665.
[43] A.D. Sabde, M.K. Trivedi, V. Ramachandhran, M.S. Hanra, B.M. Misra, Casting and characterization of cellulose acetate butyrate based UF membranes, Desalination 114 (1997) 223–232.
[44] Y. Yu, C. Zhao, L. Yu, P. Li, T. Wang, Y. Xu, Removal of perfluorooctane sulfonates from water by a hybrid coagulation–nanofiltration process, Chem. Eng. J. 289 (2016) 7–16.
[45] P. Kanagaraj, A. Nagendran, D. Rana, T. Matsuura, Separation of macromolecular proteins and removal of humic acid by cellulose acetate modified UF membranes, Int. J. Biol. Macromol. 89 (2016) 81–88.
[46] M.L.P. Ramos, J.A. González, S.G. Albornoz, C.J. Pérez, M.E. Villanueva, S.A. Giorgieri, G.J. Copello, Chitin hydrogel reinforced with TiO2 nanoparticles as an arsenic sorbent, Chem. Eng. J. 285 (2016) 581–587.
[47] B.K. Jung, J.W. Jun, Z. Hasan, S.H. Jhung, Adsorptive removal of p-arsanilic acid from water using mesoporous zeolitic imidazolate framework-8, Chem. Eng. J. 267 (2015) 9–15.
[48] G.S. Ibrahim, A.M. Isloor, A. Moslehyani, A. Ismail, Bio-inspired, fouling resistant, tannic acid functionalized halloysite nanotube reinforced polysulfone loose nanofiltration hollow fiber membranes for efficient dye and salt separation, J. Water Process Eng. 20 (2017) 138–148.
[49] Z. Wang, H. Yu, J. Xia, F. Zhang, F. Li, Y. Xia, Y. Li, Novel GO-blended PVDF ultrafiltration membranes, Desalination 299 (2012) 50–54.
[50] M.C. Nayak, A.M. Isloor, A. Moslehyani, A.F. Ismail, Preparation and characterization of PPSU membranes with BiOCl nanowafers loaded on activated charcoal for oil in water separation, J. Taiwan Inst. Chem. Eng. 77 (2017) 293–301.
[51] Y. Ma, F. Shi, Z. Wang, M. Wu, J. Ma, C. Gao, Preparation and characterization of PSf/clay nanocomposite membranes with PEG 400 as a pore forming additive, Desalination 286 (2012) 131–137.
[52] J.-J. Qin, M.H. Oo, Y.-M. Cao, L.-S. Lee, Development of a LCST membrane forming system for cellulose acetate ultrafiltration hollow fiber, Sep. Purif. Technol. 42 (2005) 291–295.
[53] I.H. Huisman, P. Prádanos, A. Hernández, The effect of protein–protein and protein–membrane interactions on membrane fouling in ultrafiltration, J. Membr. Sci. 179 (2000) 79–90.
[54] S. Ortega-Requena, S. Rebouillat, Retracted Article: bigger data open innovation: potential applications of value-added products from milk and sustainable valorization of by-products from the dairy industry, Green Chem. 17 (2015) 5100–5113.
[55] A. Rahimpour, S.S. Madaeni, Polyethersulfone (PES)/cellulose acetate phthalate (CAP) blend ultrafiltration membranes: preparation, morphology, performance and antifouling properties, J. Membr. Sci. 305 (2007) 299–312.
[56] G. Dorra, K. Ines, B.S. Imen, C. Laurent, A. Sana, T. Olfa, C. Pascal, J. Thierry, L. Ferid, Purification and characterization of a novel high molecular weight alkaline protease produced by an endophytic Bacillus halotolerans strain CT2, Int. J. Biol. Macromol. 111 (2018) 342–351.
[57] K.C. Khulbe, B. Kruczek, G. Chowdhury, S. Gagne, T. Matsuura, S.P. Verma, Characterization of membranes prepared from PPO by Raman scattering and atomic force microscopy, J. Membr. Sci. 111 (1996) 57–70.
[58] S. Chatterjee, S. De, Adsorptive removal of fluoride by activated alumina doped cellulose acetate phthalate (CAP) mixed matrix membrane, Sep. Purif. Technol. 125 (2014) 223–238.
[59] J. Zhang, Z. Xu, W. Mai, C. Min, B. Zhou, M. Shan, Y. Li, C. Yang, Z. Wang, X. Qian, Improved hydrophilicity, permeability, antifouling and mechanical performance of PVDF composite ultrafiltration membranes tailored by oxidized low-dimensional carbon nanomaterials, J. Mater. Chem. A 1 (2013) 3101–3111.
[60] Y.E. Greish, M.A. Meetani, E.A. Al Matroushi, B. Al Shamsi, Effects of thermal and chemical treatments on the structural stability of cellulose acetate nanofibers, Carbohydr. Polym. 82 (2010) 569–577.
[61] B. Ding, E. Kimura, T. Sato, S. Fujita, S. Shiratori, Fabrication of blend biodegradable nanofibrous nonwoven mats via multi-jet electrospinning, Polymer 45 (2004) 1895–1902.
[62] J.H. Ryu, H. Lee, Y.J. Kim, Y.S. Kang, H.S. Kim, Facilitated olefin transport by reversible olefin coordination to silver ions in a dry cellulose acetate membrane, Chem. Eur. J. 7 (2001) 1525–1529.
[63] L. Manjunath, R.R.N. Sailaja, PMMA–cellulose acetate phthalate nanocomposites reinforced with silane-treated nanoclay, Cellulose 21 (2014) 1793–1802.
[64] R. Ravikumar, M. Ganesh, U. Ubaidulla, E.Y. Choi, H.T. Jang, Preparation, characterization, and in vitro diffusion study of nonwoven electrospun nanofiber of curcumin-loaded cellulose acetate phthalate polymer, Saudi Pharm. J. 25 (2017) 921–926.

[65] Q. Xu, M. Zeng, Z. Feng, D. Yin, Y. Huang, Y. Chen, C. Yan, R. Li, Y. Gu, Understanding the effects of carboxylated groups of functionalized graphene oxide on the curing behavior and intermolecular interactions of benzoxazine nanocomposites, RSC Adv. 6 (2016) 31484–31496.
[66] Y. Mo, A. Tiraferri, N.Y. Yip, A. Adout, X. Huang, M. Elimelech, Improved antifouling properties of polyamide nanofiltration membranes by reducing the density of surface carboxyl groups, Environ. Sci. Technol. 46 (2012) 13253–13261.
[67] A.K. Shukla, J. Alam, M. Alhoshan, L.A. Dass, M.R. Muthumareeswaran, Development of a nanocomposite ultrafiltration membrane based on polyphenylsulfone blended with graphene oxide, Sci. Rep. 7 (2017) 41976.
[68] A.K. Shukla, J. Alam, M. Alhoshan, L.A. Dass, F.A.A. Ali, U. Mishra, M.A. Ansari, Removal of heavy metal ions using a carboxylated graphene oxide-incorporated polyphenylsulfone nanofiltration membrane, Environ. Sci.: Water Res. Technol. 4 (2018) 438–448.
[69] M.-C. Shih, An overview of arsenic removal by pressure-drivenmembrane processes, Desalination 172 (2005) 85–97.
[70] P. Bahmani, A. Maleki, R. Rezaee, M. Khamforosh, K. Yetilmezsoy, S.D. Athar, F. Gharibi, Simultaneous removal of arsenate and nitrate from aqueous solutions using micellar-enhanced ultrafiltration process, J. Water Process Eng. 27 (2019) 24–31.
[71] R. Mukherjee, S. De, Adsorptive removal of phenolic compounds using cellulose acetate phthalate–alumina nanoparticle mixed matrix membrane, J. Hazard. Mater. 265 (2014) 8–19.
[72] C.P. Durthi, S.B. Rajulapati, A.A. Palliparambi, A.K. Kola, S.H. Sonawane, Studies on removal of arsenic using cellulose acetate–zinc oxide nanoparticle mixed matrix membrane, Int. Nano Lett. 8 (2018) 201–211.